Accelerating antimalarial drug discovery with a new high-throughput screen for fast-killing compounds

Takaya Sakura[1,2,†], Ryuta Ishii[3,4,†], Eri Yoshida[1], Kiyoshi Kita[2,5,6], Teruhisa Kato[4,7], Daniel Ken Inaoka[1,2,5,6,*]

[1]Department of Molecular Infection Dynamics, Institute of Tropical Medicine (NEKKEN), Nagasaki University, Nagasaki 852-8523, Japan. [2]School of Tropical Medicine and Global Health, Nagasaki University, Sakamoto, Nagasaki 852-8523, Japan. [3]Department of Cellular Architecture Studies, Institute of Tropical Medicine (NEKKEN), Nagasaki University, Nagasaki 852-8523, Japan. [4]Laboratory for Drug Discovery and Disease Research, Shionogi & Co., Ltd., Osaka, 561-0825, Japan. [5]Department of Infection Biochemistry, Institute of Tropical Medicine (NEKKEN), Nagasaki University, Nagasaki 852-8523, Japan. [6]Department of Biomedical Chemistry, Graduate School of Medicine, The University of Tokyo, Tokyo 113-0033, Japan. [7]Exploratory Research for Drug Discovery, Institute of Tropical Medicine (NEKKEN), Nagasaki University, Nagasaki 852-8523, Japan.

[†] These authors contributed equally to this work.

*Correspondence: Daniel Ken Inaoka, danielken@nagasaki-u.ac.jp. Department of Infection Biochemistry, Institute of Tropical Medicine (NEKKEN), Nagasaki University, 1-12-4, Sakamoto,

19 Nagasaki 852-8523, Japan.

Abstract

The urgent need for rapidly acting compounds in the development of antimalarial drugs underscores the significance of such compounds in overcoming resistance issues and improving patient adherence to antimalarial treatments. The present study introduces a high-throughput screening (HTS) approach using 1536-well plates, employing *Plasmodium falciparum* lactate dehydrogenase (PfLDH) combined with nitroreductase (NTR) and fluorescent probes to evaluate inhibition of the growth of the asexual blood stage of malaria parasites. This method was adapted to efficiently measure the parasite reduction ratio (PRR) in a 384-well plate format, streamlining the traditionally time-consuming screening process. By successfully screening numerous compounds, this approach identified fast-killing hits early in the screening process, addressing challenges associated with artemisinin-based combination therapies. The high-throughput PRR method is expected to be of value in continuously monitoring fast-killing properties during structure-activity relationship studies, expediting the identification and development of novel, rapidly acting antimalarial drugs within phenotypic drug discovery campaigns.

Keywords: malaria, drug discovery, high-throughput screening, lactate dehydrogenase, nitroreductase, fast-killing,

38 **Introduction**

39 Malaria is a parasitic disease caused by *Plasmodium* spp. infection, and typically is seen in
40 tropical and subtropical areas. In 2021, over 420,000 deaths, predominantly among children
41 under 5 years old, were reported worldwide, along with more than 200 million cases[1].
42 Artemisinin-based combination therapies (ACTs) are common treatments for malaria in
43 endemic areas. Unfortunately, artemisinin-resistant parasites have spread across Southeast Asia
44 and Africa, highlighting the need for new antimalarial drugs to combat this life-threatening
45 parasitic disease[2–4]. In the last decade, the combination of phenotypic screening, and *in vitro*
46 evolution and whole-genome analysis (IVIEWGA) has played a significant role in antimalarial
47 drug development. This approach has contributed to the identification of several novel drug
48 targets for malarial parasites, facilitating target-based HTS campaigns [5,6]. Despite the strong
49 efforts in target-based drug discovery being conducted by the Medicines for Malaria Venture
50 (MMV) and collaborating researchers, the development of novel antimalarial medicines often
51 has been hampered by resistance of the malarial parasites to the drug candidates. For example,
52 recrudescent parasites emerged in Phase II clinical trials of both of DSM265 and cipargamin that
53 targets dihydroorotate dehydrogenase (DHODH) and the *Plasmodium falciparum* Na^+ pump
54 PfATP4, respectively[7–9]. Although target-based drug discovery is an effective method for
55 generating lead compounds, the targets identified by IVIEWGA carry the risk of potential

56 resistance, a major concern in the later stages of drug development. Therefore, there has been
57 renewed interest in phenotypic screening, with several of the resulting candidates now listed in
58 the current drug development pipeline of MMV.

59 Single-exposure radical cures (SERCs) are highly appealing, since this strategy
60 prevents parasite resistance and simplifies patients' treatment. However, SERCs
61 characteristically require fast-killing, as seen in next-generation lead compounds such as
62 MMV688533, INE963, ZY19489, and GSK484, the subjects of ongoing clinical trials[10–13]. The
63 standard method employed to determine the speed of killing of parasites, the parasite reduction
64 ratio (PRR), first was described in 2012; since then PRR has been utilized widely to assess the
65 killing properties of candidate compounds[14,15]. The conventional PRR assay has a relatively low
66 throughput due to the complexity of the protocol, requiring at least one month to yield results.
67 This aspect means that one cannot determine whether a given hit compound is a fast killer until
68 the candidate selection step in the drug development pipeline. Despite the crucial importance of
69 the PRR properties of next-generation lead compounds, no scalable assay method for
70 determining the PRR values of multiple compounds has been reported to date.

71 Phenotypic screening of the asexual blood stage (ABS) of malaria parasites often
72 employs the *P. falciparum* lactate dehydrogenase (PfLDH) assay to quantify parasite growth[16].
73 Specifically, PfLDH (in the lysate of a parasite culture) is coupled to the *Clostridium kluyveri*

74 diaphorase; the bacterial enzyme catalyzes a redox reaction that converts nitroblue tetrazolium
75 (NBT) to nitroblue formazan (NBF) via 3-acetyl pyridine adenine dinucleotide ($APAD^+$), a
76 nicotinamide adenine dinucleotide (NAD^+) analogue that exhibits cofactor specificity for PfLDH.
77 In the past, GlaxoSmithKline (GSK) employed the PfLDH assay to screen approximately 2 million
78 compounds in a 384-well plate format. However, of late, the SYBR green I-based fluorescence
79 assay, which detects parasite DNA, has become more commonly used for phenotypic HTS of the
80 ABS of malaria parasites. This shift occurred because the fluorescence assay was the only
81 method available for use in the 1536-well format[17,18]. Nevertheless, the simple principle of a
82 PfLDH assay that involves a redox enzyme and a detection probe coupled with the LDH reaction,
83 allows for easy tuning of the assay protocol depending on the specific purpose of the experiment.
84 In the present report, we describe the development of a modified PfLDH assay using
85 the nitroreducatase (NTR) encoded by the *Escherichia coli nfsB* gene. NTR, a flavoprotein, uses
86 NAD(P)H as an electron donor to reduce a variety of nitroaromatics[19]. To enhance the
87 conventional PfLDH assay's performance, we incorporated into the assay system "turn-on"
88 fluorescence probes that include a nitrobenzyl moiety[20,21] that is reduced by NTR. The use of a
89 near-infrared (NIR) probe with an extended wavelength range (excitation/emission
90 wavelengths ($\lambda_{ex/em}$) = 615/690 nm) compared to haemoglobin absorption (~600 nm)
91 effectively decreased interference from haemoglobin absorption in the lysate, resulting in an

92 increased signal window. This innovative approach using the NIR probe enabled us to conduct
93 phenotypic screening of the ABS of malaria in a 1536-well format, and improved the assay
94 robustness compared to that of the conventional SYBR green I assay. Moreover, the use of the
95 optimized PfLDH-NTR assay system streamlined the time-consuming protocol of conventional
96 PRR. A feasibility study with representative antimalarial drugs showed results consistent with
97 those obtained using the conventional PRR method. Our high-throughput PRR (HT-PRR) assay
98 therefore is expected to serve as a powerful tool for identifying, in the early stages of drug
99 discovery, novel antimalarial compounds with fast-killing profiles.
100

101 **Results**

102 **Coupling of NTR reaction with PfLDH**

103 Histidine-tagged NTR expressed in *E. coli* was purified successfully using conventional nickel-
104 nitrilotriacetic acid (Ni-NTA) agarose purification, yielding a specific activity in the range of 3–5
105 μmol/min/mg (Fig. 1a). The recombinant NTR converted nitrobenzyl-umbelliferone 1 (NCOU1)
106 to umbelliferone, such that the fluorescent signal of the product ($\lambda_{ex/em}$ = 315/455 nm) exhibited
107 a time-dependent increase during room temperature incubation (Fig. 1b, c). For our assay, PfLDH
108 was coupled with the purified NTR, rather than with the bacterial diaphorase used in the
109 conventional PfLDH assay, and parasite growth was quantified by monitoring the fluorescence

110 signal of umbelliferone (Fig. 2a). As anticipated, the NTR quantitatively reduced NCOU1 by using
111 the reducing equivalents from the APADH produced by the PfLDH enzyme present in the parasite
112 lysate. A titration of cultured *P. falciparum* using the PfLDH-NTR assay demonstrated that the
113 fluorescent signal increased in a parasitemia-dependent manner, with the highest signal
114 intensity seen under the condition of 1% haematocrit (Fig. 2b and Supplementary Fig. 1).

115 Next, we compared the screening performance, in a 384-well plate format, of the
116 PfLDH-NTR assay compared to the conventional PfLDH-diaphorase assay. Specifically, we used
117 the two assays to assess the growth inhibition of ABS parasites by a test set of 3,837 compounds
118 from Shionogi & Co., Ltd., using a compound concentration of 2.5 μM. A correlation (r^2 = 0.387)
119 was observed between the results obtained by the two methods, as depicted in Fig. 2c. While the
120 average signal-to-background (S/B) ratio for the NTR method (5.02) was lower than that of the
121 diaphorase method (8.31), the two assays demonstrated similar Z'-factor values (0.71 and 0.76,
122 respectively) (Table 1). Notably, the diaphorase method produced a higher number of hits (261
123 hits) than did the NTR method (123 hits). The PfLDH-diaphorase method may have selected for
124 a larger number of pseudo-positive hits, given that this assay's percent inhibition data did not
125 exhibit a Gaussian distribution and did not correlate with data obtained by other methods
126 (Supplementary Fig. 2, 3, 4). These results indicated that our fluorescence-based PfLDH assay,
127 which incorporates NTR and NCOU1, is more robust than the conventional PfLDH assay using

128 diaphorase.

129

130 **NIR probe with PfLDH-NTR assay improves screening robustness**

131 The PfLDH-NTR-NCOU1 assay was not suitable for a 1536-well format due to the low S/B ratio.
132 Consequently, our next objective was to improve this assay method using another probe with a
133 different wavelength of fluorescence emission. Given that the parasite lysate contains a
134 substantial amount of haemoglobin from red blood cells, we conjectured that the absorption of
135 haemoglobin (~600 nm) interferes with the fluorescent signal of umbelliferone[20]. Therefore, we
136 introduced another NIR probe, one that exhibits longer excitation and emission wavelengths
137 after reduction by NTR (Fig. 3a). We observed that, following reduction of the NIR probe by NTR
138 in the assay solution, the signal intensity of the reduced species (NIR-P^{red}), increased in a time-
139 dependent manner, permitting quantification of the malaria parasites (Fig. 3b, c). Given the read-
140 time need for measurement of output in the 1536-well format, we quenched the PfLDH reaction
141 by adding a high concentration of pyruvate (0.9 M), resulting in the complete inhibition of
142 NCOU1 reduction (Fig 3c). For reactions run in the 1536-well format, the parasite growth
143 inhibition detected by the PfLDH-NTR-NIR assay showed a strong correlation with that obtained
144 by the SYBR green I-based assay (Fig. 3d). Notably, the PfLDH-NTR-NIR assay achieved a higher
145 S/B ratio and Z'-factor (11.2 and 0.72, respectively) than those measured by the SYBR green I

146 assay (5.89 and 0.61), indicating that PfLDH-NTR-NIR assay is more robust than the existing

147 method when employed in a 1536-well format.

148

149 **High-throughput PRR (HT-PRR) assay**

150 In the ABS, LDH oxidizes NADH and provides NAD^+ to maintain the flux of anaerobic glycolysis

151 required for the synthesis of ATP, a function that is essential for parasite survival[22,23]. We

152 conceived the idea of using PfLDH activity as an indicator of parasite viability and applied the

153 PfLDH-NTR-NCOU1 method in a 384-well format to quantify the PRRs of test compounds. Mixed-

154 stage (non-synchronized) parasites at 1.5% parasitemia were incubated at 37 °C for 0, 24, 48,

155 72, and 96 hours with test compounds at concentrations of 10 μM. Live parasite signals were

156 quantified by the PfLDH-NTR-NCOU1 method and the PRR values were calculated for each

157 compound. The values then were normalized (as a percentage) to those of dihydroartemisinin

158 (DHA; defined as 100%), a representative fast-killing compound, and ELQ300 (defined as 0%),

159 an inhibitor of the electron transport chain (ETC) that is classified as a slow-killing compound

160 (Supplementary Fig. 5). At 24 hours, fast-killing compounds like ACT-451840, artemether, and

161 cipargamin exhibited PRR values exceeding 70%; chloroquine, MMV048, and ganaplacide,

162 categorized as moderate-speed-killing compounds, yielded PRR values in the approximate range

163 of 40–70%. Other known slow-killing ETC inhibitors, DSM265 and atovaquone, yielded lower

164 PRR values (16.9 and 8.6%, respectively). These results are consistent with the data obtained by
165 the conventional PRR method. The sole exception was DDD107498, a compound known to be a
166 slow-killing inhibitor by conventional PRR[24], show high PRR value. Given that this compound is
167 an inhibitor of the eukaryotic translation elongation factor 2 (eEF2)[24]; we hypothesize that the
168 interruption of protein synthesis by DDD107498 may directly impact PfLDH synthesis, leading
169 to lowered enzymatic activity, which our assay detects as an elevated PRR.

170 Subsequently, we sought to optimize the level of parasitemia in the assay by employing
171 our method to assess the effects, on parasites at various densities, of 24- and 48-hour exposure
172 to the known inhibitors atovaquone, DHA, and cipargamin (Supplementary Fig. 6). We observed
173 that when the starting parasitemia exceeded 2%, the signal for vehicle (dimethylsulfoxide;
174 DMSO)-treated parasites achieved a virtual plateau after 48 hours of incubation. Therefore, we
175 fixed the starting parasitemia at 1.5% for further experiments.

176 Having completed the optimization of HT-PRR, we conducted PRR assays in an 8-point
177 dose-response experiment. The dose-response PRR experiment was implemented because
178 during the test run, we observed that the shape of PRR dose curves differed among the
179 compounds (Supplementary Fig. 7). The experiment assessed PRR at intervals of 0, 24, 48, and
180 72 hours; and determined the 50% effective concentration to reduce the PRR values (PRR_{50}) of
181 the representative test compounds, in addition to the 72-hour cultures for standard growth

182 inhibition (EC_{50}) assays (Fig. 4a). A comparison of the inhibition curves revealed that Hill slopes
183 and plateau levels of the PRR curves varied among compounds and time points. To quantify the
184 shape of the dose-response curve and utilize these data as an indicator of PRR, we calculated for
185 each compound the ratio of area under the curve (AUC) between the growth inhibition curve
186 and the PRR curve, yielding a parameter that we refer to as the "AUC%" (Table 2). We observed
187 that the AUC% values of the fast-killing compounds exceeded 80%. In contrast, the slow-killing
188 compound exhibited lower AUC% values (of approximately 50%); furthermore, the % inhibition
189 by slow-killing compounds did not reach 100%, even at the highest tested concentration (1 μM).
190 These data suggested that robust AUC% values, calculated using multiple data points, permitted
191 effective classification of compounds according to their killing-rate properties.
192
193 **Discussion**
194 In the present work, we established a novel PfLDH-based assay method for detecting
195 antimalarial candidates targeting the ABS by using NTR and "turn-on" fluorescent probes with a
196 nitrobenzyl moiety. The new method provides an assay with robustness superior to that of
197 existing screening methods, and we successfully conducted HTS with a small compound library
198 in a 1536-well format. Our method also was able to assess the parasite survival rate, as assessed
199 by PfLDH activity. The PfLDH-NTR assay permits quantification of the PRR for many compounds

200 in a 384-well format, significantly decreasing experimental time. The PRR classification of
201 known antimalarial drugs by our HT-PRR method was consistent with the data obtained by
202 conventional assays. Moreover, HT-PRR permitted the determination of the dose-dependency of
203 a compound's PRR, yielding a new parameter (the AUC%) indicating the speed of killing. Our
204 novel PfLDH-NTR-based assay is expected to be valuable for determining the PRR values of many
205 hit compounds in the early stages of drug discovery, facilitating the development of next-
206 generation fast-killing antimalarial drugs.

207 In the field of cancer research, NTR is widely used for the *in vivo* detection of tumour
208 cells and the activation of prodrugs, reflecting the fact that NTR expression is specifically
209 increased in tumour cells growing under hypoxic conditions[25–27]. Additionally, NTR plays a
210 crucial role in the treatment of Chagas disease, a condition caused by *Trypanosoma cruzi*
211 infection; benznidazole and nifurtimox, front-line drugs used against Chagas, are activated by
212 NTR activity. Resistance to these drugs is determined primarily by loss of function mutations in
213 the *T. cruzi* NTR-encoding gene (including homozygous nonsense mutations and the loss of one
214 copy) that lead to decreased levels of the trypanosomal enzyme[28,29]. Given NTR's biological
215 significance and diverse applications in biomedical research, we envisioned using NTR to
216 establish innovative assays for the discovery of antimalarial drugs. Moreover, the tissue
217 transparency of the $\lambda_{ex/em}$ of NIR, which fall within the bio-optical window (650–1100 nm),

218 makes these wavelengths useful in biomedical research, especially for *in vivo* imaging, due to
219 lower haemoglobin absorption[30]. This property of the NIR probe fluorophore mitigates
220 interference from the abundant haemoglobin in red blood cells, greatly enhancing the signal
221 strength of the PfLDH assay. Through the introduction of a coupling enzyme and probes, we
222 improved the performance of the conventional PfLDH assay for detecting growth inhibition of
223 the malaria parasite at the ABS. In the future, it will be interesting to introduce modifications to
224 existing assay systems, thereby enhancing robustness and reducing cost. This initiative has the
225 potential to pave the way for the creation of advanced HTS systems applicable to other infectious
226 diseases, including *Trypanosoma* spp. and *Mycobacteria* spp.; indeed, revisions to facilitate
227 screens for these systems are currently in progress.

228 For HTS of the ABS of the malaria parasite in a 1536-well format, the commonly used
229 assay employs SYBR green I, a fluorescent dye with excitation and emission wavelengths of 485
230 nm and 528 nm, respectively. Our PfLDH-NTR assay with NIR^{ox} would be (to our knowledge) the
231 first system using NIR wavelengths to screen for antimalarial compounds. A noteworthy finding
232 is that a small number of hit compounds of the SYBR green I-based assay was not common with
233 that of the PfLDH-NTR with NIR^{ox} assay (Supplementary Fig. 4). The optical properties of small
234 organic compounds in chemical libraries may impact the readout signal, resulting in false-
235 positives and -negatives[31,32]. Indeed, a small number of compounds showed less than 40%

236 inhibition as assessed by the SYBR green I-based assay, possibly reflecting the optical properties
237 of these compounds (Supplementary Fig. 2). The PfLDH-NTR with NIR^{ox} assay may serve as a
238 viable alternative screening method to prevent the loss of promising compounds as pseudo-
239 negatives in future phenotypic HTS of the malaria parasite at the ABS.

240 To enhance the throughput in assessing PRR, we developed the PfLDH-NTR assay
241 system, enabling the HTS evaluation of antimalarial compounds based on PRR values. Notably,
242 we observed that the dose dependent PRRs of fast-killing compounds typically demonstrate
243 curves that resembled the growth inhibition curve of the same chemicals. However, disparities
244 between these two types of curves are more pronounced for moderate- and slow-killing
245 compounds. To quantify these differences, and to classify multiple test compounds according to
246 the PRR value, we defined the AUC%. This parameter provides a succinct description of the
247 parasite killing rate of test compounds and is expected to accelerate structure-activity
248 relationship (SAR) studies, particularly for fast-killing compounds. At the same time, we note
249 that a limitation of HT-PRR is that PRR values for compounds targeting protein synthesis (e.g.,
250 DDD107498) may be overestimated due to the dependence of the assay on PfLDH activity.
251 However, this limitation can be addressed by cross-referencing results with conventional PRR or
252 classical Giemsa staining at later stages of drug discovery.

253

254 **Conclusion**

255 We developed, in-house, NTR-based methods for the identification of compounds with
256 activity against the ABS of malaria parasites, and successfully implemented one such assay for
257 HTS in a 1536-well format. The use of the PfLDH-NTR method for PRR determination represents
258 a novel assay of the parasite-killing rate of drug candidates. These innovative new HTS methods
259 are expected to permit the identification of fast-killing compounds with novel scaffolds and
260 properties, paving the way for the discovery of next-generation antimalarial drugs that may find
261 use in combatting drug resistance in malaria-endemic areas.
262

263 **Methods**

264 **Preparation of recombinant enzymes**

265 Prior to assay development, we prepared two coupling enzymes, *Clostridium kluyveri* diaphorase
266 and *Escherichia coli* NAD(P)H nitroreductase NfsB (NTR), as previously described[19,33]. Briefly,
267 codon-optimized genes were synthesized to encode proteins with N-terminal His10-SUMO tags
268 and C-terminal His10 tags. These genes with C-terminal His10 were cloned separately into the
269 pET101-D-TOPO expression vector (Thermo Fisher Scientific), and the resulting plasmids were
270 transformed into *E. coli* BL21™ Star (DE3) cells according to the manufacturer's protocol. The
271 resulting *E. coli* strains were pre-cultured (overnight at 37 °C with shaking at 200 rpm) in Luria–
272 Bertani medium supplemented with 100 μg/mL carbenicillin. The resulting cultures were used
273 as inocula for 600-mL volumes of Terrific-Broth medium supplemented with 100 μg/mL
274 carbenicillin and 0.4% glycerol, and the resulting cultures were incubated at 37 °C with shaking
275 at 200 rpm. When the optical density at 600 nm (OD_{600}) reached 0.4 to 0.6, protein expression
276 was induced by adding 50 μM isopropyl β-D-1-thiogalactopyranoside (IPTG; Sigma) and 1
277 mg/mL riboflavin (Sigma). After incubation for 16 h at 20 °C, the cells were harvested by
278 centrifugation at 7,000 × *g* for 10 min at 4 °C and re-suspended at a density of 0.4 g cell pellet/mL
279 in cold lysis buffer (50 mM potassium phosphate buffer, pH 8.0, 300 mM NaCl, 0.5 mM
280 ethylenediaminetetraacetic acid (EDTA) and 0.25 mM phenylmethylsulfonyl fluoride (PMSF)).
281 The suspended cells were lysed using a French press (Ohtake) at 180 MPa, and the supernatant

282 was collected by centrifugation at 40,000 × *g* for 30 min at 4 °C. The His-tagged proteins were
283 purified using Ni-NTA (Qiagen) following the manufacturer's protocol and eluted using lysis
284 buffer containing 200 mM imidazole. The eluate was concentrated using an Amicon Ultra
285 Centrifugal Filter 10 kDa Molecular Weight Cut-off (Merck) according to the manufacturer's
286 protocol, and the resulting purified enzyme was mixed with an equal volume of cold glycerol and
287 stored frozen at -30 °C. The protein concentrations in the final enzyme stocks were determined
288 by the Bradford assay using a Bio-Rad kit, and the specific activities of the enzymes were
289 quantified by measuring the reduction of 2,6-dichlorophenolindophenol (DCIP; Sigma) using a
290 UV760 spectrophotometer (Jasco). To confirm the purity of the enzymes, proteins were
291 separated by sodium dodecyl sulfate-polyacrylamide gel electrophoreses (SDS-PAGE) and
292 stained using GelCode™ Blue Safe Protein Stain (Thermo Fisher Scientific). The specific activities
293 of diaphorase and NTR were typically in the range of 100–150 and 3–5 μmol/min/mg,
294 respectively.
295
296 **Quantification of the reduction of fluorescence probes by NTR**
297 To test whether the purified NTR was capable of reducing fluorescence probes, we initially
298 measured NTR activity prior to using the enzyme for parasite quantification. Using a cuvette, 20
299 μM NCOU1 (Enamine) was combined with a mixture containing 5 μg/mL NTR, 50 μM NADH, and

300 0.25 % Triton X-100 in 30 mM Tris-HCl (pH 8.0), and the fluorescence of the umbelliferone

301 ($\lambda_{ex}/_{em}$ = 315/455 nm) generated by the reaction was measured. In addition, we synthesized the

302 NIR^{ox} probe according to the previously described route[21]. For the NIR reaction, 50 μM $NIR\text{-}P^{ox}$

303 was combined with a mixture containing 0.5 μg/mL NTR and 50 μM NADH in 30 mM Tris-HCl

304 (pH 8.0), and the fluorescence of $NIR\text{-}P^{red}$ ($\lambda_{ex}/_{em}$ = 615/670 nm) was measured. The

305 fluorescence kinetics of both reduced probes were monitored using a FP-6300

306 spectrofluorometer (Jasco).

307

308 **Parasite cultures**

309 *Plasmodium falciparum* 3D7 parasites were maintained in RPMI1640 medium supplemented

310 with 25 mg/L gentamicin, 50 mg/L hypoxanthine, 23.8 mM sodium bicarbonate, and 0.5% (w/v)

311 Albumax II (Gibco). The culture was maintained at 2% haematocrit using O^+ human erythrocytes

312 obtained from The Japanese Red Cross Society. As per established protocols[34,35], the incubation

313 temperature was set at 37 °C and the environment consisted of mixed gas (5% O_2, 5% CO_2, 90%

314 N_2). Parasitemia was determined using either Giemsa staining or an XN-30 automated

315 haematology analyser (Sysmex)[36]. For plate assays, ring-stage synchronized parasites were

316 prepared using sorbitol treatment[37]. In the growth inhibition assay, the compound solvent DMSO

317 and a mixture of 1 μM artemisinin/atovaquone served as negative and positive controls,

318 respectively.

319

320 **Diaphorase-NBT and NTR-NCOU1 assay in 384-well plates**

321 Test compounds were pre-dispensed at a volume of 100 nL/well into 384-well plates. For the
322 diaphorase-NBT assay, ring-stage parasites at 0.3% parasitemia and 2% haematocrit were
323 dispensed into 384-well clear plates (Corning); for the NTR-NCOU1 assay, ring-stage parasites
324 at 0.3% parasitemia and 1% haematocrit were dispensed into 384-well black plates (Greiner).
325 Parasites then were dispensed at 25 μL/well into the compound-containing plates using a
326 Multidrop Combi with a small metal cassette (Thermo Fisher Scientific). The parasite cultures in
327 the assay plates then were incubated in a moist chamber filled with mixed gas for 72 hours and
328 subsequently frozen overnight (or longer) at -30 °C. The resulting frozen plates were thawed at
329 room temperature for at least 2 hours before the assay was performed. For the diaphorase-NBT
330 assay, the reaction mix was prepared in modified PfLDH buffer (100 mM Tris-HCl, pH 8.0, 150
331 mM lithium L-lactate, and 0.25% Triton X-100) supplemented with 75 μM $APAD^+$, 0.2 mg/mL
332 NBT, and 1 U/mL diaphorase (one unit was defined as the amount of enzyme required to reduce
333 1 μmol of APADH per minute). For this assay, the reaction mixture was dispensed into the assay
334 plates at 70 μL/well, and the plates then were incubated at room temperature with agitation at
335 650 rpm for 20 minutes. On the other hand, the reaction mixture for the NTR-NCOU1 assay

336 consisted of modified PfLDH buffer supplemented with 100 μM $APAD^+$, 100 μM NCOU1, 0.05
337 U/mL NTR, and 0.015% (v/v) KM-70 defoaming agent (Shin-Etsu). For this assay, the reaction
338 mix was dispensed into the assay plates at 35 μL/well, and the plates then were incubated under
339 the same condition as those used for the diaphorase-NBT assay. The absorption of nitro blue
340 formazan (650 nm; for the diaphorase-NBT assay) or the fluorescence of umbelliferone ($\lambda_{ex/em}$ =
341 360/465 nm; for the NTR-NCOU1 assay) was measured using a SpectraMax® Paradigm
342 spectrophotometer (Molecular Devices, Inc.).
343
344 **NTR-NIR^{ox} assay in 1536-well plates**
345 For the HTS in 1536-well format, ring-stage parasites at 0.3% parasitemia and 1%
346 haematocrit were dispensed at 4 μL/well into 1536-well black plates (Greiner) containing 20
347 nL/well of test compounds. Parasite-dispensed assay plates were maintained under the same
348 conditions as described above for the 384-well plate assays. The NIR^{ox} probe was initially
349 suspended at 1 mM in 90% acetonitrile. The reaction mixture for the NTR-NIR^{ox} assay was
350 prepared by supplementing modified PfLDH buffer with 500 μM $APAD^+$, 200 μM NIR^{ox} probe,
351 and 0.05 U/mL NTR. For this assay, the reaction mixture was dispensed into the assay plates at
352 3 μL/well, and the contents of each well were mixed at 1,200 rpm. The plates then were
353 incubated at room temperature for 3 minutes. The enzymatic reactions were quenched by

354 dispensing the "stop" mixture (0.9 M sodium pyruvate containing 0.015% KM-70) at 3 μL/well,
355 and the assay plates then were centrifuged at 90 × *g* for 1 min at room temperature. The
356 centrifuged plates were incubated for 1 hour at room temperature in a moist chamber, at which
357 point the NIR^{red} signal ($\lambda_{ex/em}$ = 615/690 nm) was measured using a PHERAstar Plus microplate
358 reader (BMG LABTECH).
359
360 **SYBR green assay in 1536-well plates**
361 For the SYBR green assay, ring-stage parasites at 0.3% parasitemia and 3% haematocrit were
362 dispensed at 4 μL/well into 1536-well black plates (Greiner) containing 20 nL/well of test
363 compounds. Parasite-dispensed assay plates were maintained under the same conditions as
364 described above for the 384-well plate assays. The reaction mixture for the SYBR green I assay
365 consisted of lysis buffer (20 mM Tris-HCl, pH 8.0, 5 mM EDTA, and 0.1% Triton X-100)
366 supplemented with 0.02% SYBR green I and 0.015% KM-70. This reaction mixture was
367 dispensed into the assay plates at 4 μL/well, and the contents of each well were mixed at 1,200
368 rpm. The plates then were incubated at room temperature for 1 hour. The fluorescence of SYBR
369 green I ($\lambda_{ex}/_{em}$ = 485/528 nm) was measured using a SpectraMax® Paradigm
370 spectrophotometer.
371

372 **Data analysis**

373 Hits of a test set of compounds were chosen by activity criteria [>3 standard deviation (SD)
374 cutoff of DMSO controls] that were calculated using Spotfire software (version 11.4.3; TIBCO). Z'
375 was calculated as $1 - (3 \times SD_{100\%} + 3 \times SD_{0\%})/(Mean_{100\%} - Mean_{0\%})$. The correlations
376 of %Inhibition and histograms were visualized with R (version 4.0.2). The inhibition curves and
377 EC_{50} values were determined using GraphPad Prism (version 8.4.3. GraphPad Software, Inc., San
378 Diego, California, USA) and Spotfire. Data visualization for the other figures was performed using
379 GraphPad Prism. The area under the curve (AUC) for both the HT-PRR assay and growth
380 inhibition assay in the 384-well plates was calculated using Spotfire software, and the AUC% was
381 calculated as 100 × [(AUC of HT-PRR assay) / (AUC of NTR-NCOU1 assay)]. Venny (version 2.1)
382 was used to make a Venn diagram.

383

384 **HT-PRR assay in 384-well plates**

385 Test compounds were pre-dispensed at 100 nL/well in 384-well plates, and replicate plates were
386 prepared. Non-synchronized parasites at 1.5% parasitemia and 1% haematocrit were dispensed
387 into five 384-well black compound-containing plates at 25 μL/well using a Multidrop Combi
388 with a small metal cassette. One of the plates was frozen at -30 °C right immediately following
389 dispensing of parasites (control plate; 0 hour), while the other plates were incubated in a moist

390 chamber filled with mixed gas for 24, 48, 72, or 96 hours; at the indicated time points, growth
391 was terminated by freezing overnight (or longer) at -30 °C (PRR plates). Additional plates for the
392 generation of the growth inhibition curve were prepared and subjected to the NTR-NCOU1 assay
393 using the procedure described in the previous section, with a 72-hour incubation period. The
394 fluorescence of umbelliferone ($\lambda_{ex/em}$ = 360/465 nm) was measured using a PHERAstar
395 microplate reader, and the relative LDH activity was calculated by dividing the fluorescence of
396 the PRR plates by that of the respective control plate. The PRR inhibition percentage was
397 calculated by normalizing the primary values to the LDH activity obtained in the negative and
398 positive control reactions (compound solvent DMSO and 1 μM dihydroartemisinin, respectively).
399 In addition, the concentration of each compound to reduce the PRR value to 50% (PRR_{50}) was
400 calculated in each time point.
401

402 **Acknowledgements**

403 The authors thank the Japanese Red Cross Society for providing human red blood cells (RBCs;
404 Registry No. R030038) and Dr. Kenji Takaya (Laboratory for Medicinal Chemistry Research,
405 Shionogi & Co., Ltd.) for synthesizing the NIR probe.
406

407 **Abbreviations Used**

408 PfLDH, *Plasmodium falciparum* lactate dehydrogenase; NTR, nitroreductase; PRR, parasite
409 reduction ratio; ACTs, artemisinin-based combination therapies; IVIEWGA, *in vitro* evolution and
410 whole-genome analysis; MMV, Medicines for Malaria Venture; DHODH, dihydroorotate
411 dehydrogenase; SERCs, single-exposure radical cures; ABS, asexual blood stage; NBT, nitroblue
412 tetrazolium; NBF, nitroblue formazan; $APAD^+$, 3-acetyl pyridine adenine dinucleotide; NIR, near-
413 infrared; NCOU1, nitrobenzyl-umbelliferone 1; ETC, electron transport chain; DHA,
414 dihydroartemisinin; eEF2, elongation factor 2; PMSF, phenylmethylsulfonyl fluoride; DCIP, 2,6-
415 dichlorophenolindophenol
416

417 **Fundings**

418 This work was supported, in part, by the following funding sources: grants for Infectious Disease
419 Control from the Science and Technology Research Partnership for Sustainable Development
420 (SATREPS; No. JP10000284 to K.K., and No. JP14425718 to D.K.I. and T.S.); grants from the
421 Agency for Medical Research and Development (AMED); Grants-in-aid for Scientific Research (A)
422 (No. 20H00620 to D.K.I.), (B) (23H02711 to K.K. and D.K.I.), and (C) (No. JP22512047 to T.S.); a
423 grant from The Leading Initiative for Excellent Young Researchers (LEADER; No. JP16811362 to
424 D.K.I.) from the Japanese Ministry of Education, Science, Culture, Sports and Technology (MEXT);
425 and by Grants-in-aid for Research on Emerging and Re-emerging Infectious Diseases from the

Japanese Ministry of Health and Welfare (No. 21fk0108138 and No. 23fk0108680 to D.K.I.). This work also was supported by Shionogi & Co., Ltd., Osaka, Japan.

Author contributions

D.K.I., T.K., and K.K. directed the work. T.S., R.I., and E.Y. performed the experiments. T.S., R.I., and E.Y. analysed the data. T.S., R.I., E.Y., and D.K.I. wrote the paper. All authors directly participated in this work, including preparation of the manuscript and approval of the final version. All authors have read and agreed to the published version of the manuscript.

Conflict of interest

RI and TK are employees of Shionogi & Co., Ltd..

Nagasaki University and Shionogi & Co., Ltd., launched the Shionogi Global Infectious Division (SHINE) at the Institute of Tropical Medicine NEKKEN, Nagasaki University. Under the collaboration agreement, Shionogi & Co., Ltd. provided the NIR-P reagent and compounds pre-dispensed into the 384- and 1536-well plates for validation of HTS, and contributed to discussions with the authors. Shionogi & Co., Ltd did not influence the experimental design, data collection, data analysis, or interpretation.

443 **References**

444 1. World Health Organization. *World malaria report 2022*. (World Health Organization, 2022).

445 2. Ariey, F. *et al.* A molecular marker of artemisinin-resistant Plasmodium falciparum malaria.
446 *Nature* **505**, 50–55 (2014).

447 3. Mbengue, A. *et al.* A molecular mechanism of artemisinin resistance in Plasmodium
448 falciparum malaria. *Nature* **520**, 683–687 (2015).

449 4. Balikagala, B. *et al.* Evidence of Artemisinin-Resistant Malaria in Africa. *N. Engl. J. Med.* **385**,
450 1163–1171 (2021).

451 5. Cowell, A. N. *et al.* Mapping the malaria parasite druggable genome by using in vitro
452 evolution and chemogenomics. *Science* **359**, 191–199 (2018).

453 6. Siqueira-Neto, J. L. *et al.* Antimalarial drug discovery: progress and approaches. *Nat. Rev.*
454 *Drug Discov.* **22**, 807–826 (2023).

455 7. Llanos-Cuentas, A. *et al.* Antimalarial activity of single-dose DSM265, a novel plasmodium
456 dihydroorotate dehydrogenase inhibitor, in patients with uncomplicated Plasmodium
457 falciparum or Plasmodium vivax malaria infection: a proof-of-concept, open-label, phase 2a
458 study. *Lancet Infect. Dis.* **18**, 874–883 (2018).

459 8. Schmitt, E. K. *et al.* Efficacy of Cipargamin (KAE609) in a Randomized, Phase II Dose-
460 Escalation Study in Adults in Sub-Saharan Africa With Uncomplicated Plasmodium

461 falciparum Malaria. *Clin. Infect. Dis.* **74**, 1831–1839 (2022).

462 9. Yang, T. *et al.* MalDA, Accelerating Malaria Drug Discovery. *Trends Parasitol.* **37**, 493–507

463 (2021).

464 10. Murithi, J. M. *et al.* The antimalarial MMV688533 provides potential for single-dose cures

465 with a high barrier to Plasmodium falciparum parasite resistance. *Sci. Transl. Med.* **13**,

466 (2021).

467 11. Taft, B. R. *et al.* Discovery and Preclinical Pharmacology of INE963, a Potent and Fast-Acting

468 Blood-Stage Antimalarial with a High Barrier to Resistance and Potential for Single-Dose

469 Cures in Uncomplicated Malaria. *J. Med. Chem.* **65**, 3798–3813 (2022).

470 12. Barber, B. E. *et al.* Safety, pharmacokinetics, and antimalarial activity of the novel

471 triaminopyrimidine ZY-19489: a first-in-human, randomised, placebo-controlled, double-

472 blind, single ascending dose study, pilot food-effect study, and volunteer infection study.

473 *Lancet Infect. Dis.* **22**, 879–890 (2022).

474 13. Gomes, P. & Guido, R. V. C. Editorial: Antimalarial chemotherapy in the XXIst century, volume

475 II. *Front. Pharmacol.* **14**, 1229764 (2023).

476 14. Sanz, L. M. *et al.* P. falciparum in vitro killing rates allow to discriminate between different

477 antimalarial mode-of-action. *PLoS One* **7**, e30949 (2012).

478 15. Walz, A. *et al.* The Parasite Reduction Ratio (PRR) Assay Version 2: Standardized

Assessment of Plasmodium falciparum Viability after Antimalarial Treatment In Vitro. *Pharmaceuticals* **16**, (2023).

16. Makler, M. T. & Hinrichs, D. J. Measurement of the lactate dehydrogenase activity of Plasmodium falciparum as an assessment of parasitemia. *Am. J. Trop. Med. Hyg.* **48**, 205–210 (1993).
17. Gamo, F.-J. *et al.* Thousands of chemical starting points for antimalarial lead identification. *Nature* **465**, 305–310 (2010).
18. Smilkstein, M., Sriwilaijaroen, N., Kelly, J. X., Wilairat, P. & Riscoe, M. Simple and inexpensive fluorescence-based technique for high-throughput antimalarial drug screening. *Antimicrob. Agents Chemother.* **48**, 1803–1806 (2004).
19. Zenno, S., Koike, H., Tanokura, M. & Saigo, K. Gene cloning, purification, and characterization of NfsB, a minor oxygen-insensitive nitroreductase from Escherichia coli, similar in biochemical properties to FRase I, the major flavin reductase in Vibrio fischeri. *J. Biochem.* **120**, 736–744 (1996).
20. Sedgwick, A. C. *et al.* A simple umbelliferone based fluorescent probe for the detection of nitroreductase. *Frontiers of Chemical Science and Engineering* **12**, 311–314 (2018).
21. Shi, Y., Zhang, S. & Zhang, X. A novel near-infrared fluorescent probe for selectively sensing nitroreductase (NTR) in an aqueous medium. *Analyst* **138**, 1952–1955 (2013).

497 22. Zhang, M. *et al.* Uncovering the essential genes of the human malaria parasite Plasmodium
498 falciparum by saturation mutagenesis. *Science* **360**, (2018).
499 23. Shoemark, D. K., Cliff, M. J., Sessions, R. B. & Clarke, A. R. Enzymatic properties of the lactate
500 dehydrogenase enzyme from Plasmodium falciparum. *FEBS J.* **274**, 2738–2748 (2007).
501 24. Baragaña, B. *et al.* A novel multiple-stage antimalarial agent that inhibits protein synthesis.
502 *Nature* **522**, 315–320 (2015).
503 25. Li, Y. *et al.* Ultrasensitive near-infrared fluorescence-enhanced probe for in vivo
504 nitroreductase imaging. *J. Am. Chem. Soc.* **137**, 6407–6416 (2015).
505 26. Chevalier, A., Zhang, Y., Khdour, O. M., Kaye, J. B. & Hecht, S. M. Mitochondrial Nitroreductase
506 Activity Enables Selective Imaging and Therapeutic Targeting. *J. Am. Chem. Soc.* **138**, 12009–
507 12012 (2016).
508 27. Copp, J. N. *et al.* Engineering a Multifunctional Nitroreductase for Improved Activation of
509 Prodrugs and PET Probes for Cancer Gene Therapy. *Cell Chem Biol* **24**, 391–403 (2017).
510 28. Hall, B. S., Bot, C. & Wilkinson, S. R. Nifurtimox activation by trypanosomal type I
511 nitroreductases generates cytotoxic nitrile metabolites. *J. Biol. Chem.* **286**, 13088–13095
512 (2011).
513 29. Wilkinson, S. R., Taylor, M. C., Horn, D., Kelly, J. M. & Cheeseman, I. A mechanism for cross-
514 resistance to nifurtimox and benznidazole in trypanosomes. *Proc. Natl. Acad. Sci. U. S. A.* **105**,

5022–5027 (2008).

30. Hammerich, M. *et al.* Heterodiazocines: Synthesis and Photochromic Properties, Trans to Cis Switching within the Bio-optical Window. *J. Am. Chem. Soc.* **138**, 13111–13114 (2016).

31. Joung, J. F., Han, M., Jeong, M. & Park, S. Experimental database of optical properties of organic compounds. *Sci Data* **7**, 295 (2020).

32. Simeonov, A. *et al.* Fluorescence spectroscopic profiling of compound libraries. *J. Med. Chem.* **51**, 2363–2371 (2008).

33. Chakraborty, S., Sakka, M., Kimura, T. & Sakka, K. Cloning and expression of a Clostridium kluyveri gene responsible for diaphorase activity. *Biosci. Biotechnol. Biochem.* **72**, 735–741 (2008).

34. Komatsuya, K. *et al.* Siccanin Is a Dual-Target Inhibitor of Plasmodium falciparum Mitochondrial Complex II and Complex III. *Pharmaceuticals* **15**, (2022).

35. Trager, W. & Jensen, J. B. Human malaria parasites in continuous culture. *Science* **193**, 673–675 (1976).

36. Tougan, T. *et al.* An automated haematology analyzer XN-30 distinguishes developmental stages of falciparum malaria parasite cultured in vitro. *Malar. J.* **17**, 1–8 (2018).

37. Lambros, C. & Vanderberg, J. P. Synchronization of Plasmodium falciparum erythrocytic stages in culture. *J. Parasitol.* **65**, 418–420 (1979).

533 **Tables**

534 **Table 1: Parameters for each assay method**

Method	Plate format	S/B	CV (%)		Z'	Number of hits	Hit rate (%)
			Negative	Positive			
Diaphorase-NBT	384	8.31	8.1	2.6	0.71	261	6.8
NTR-NCOU1	384	5.02	5.6	3.9	0.76	123	3.2
SYBR green	1536	5.89	9.6	6.2	0.61	66	1.7
NTR-NIR	1536	11.2	8.0	6.2	0.72	70	1.8

535 NBT: nitroblue tetrazolium, NTR: nitroreductase, NCOU1: nitrobenzyl-umbelliferone 1, NIR:

536 near-infrared, S/B: signal/background ratio, CV: coefficient of variation

537

538 **Table 2: Activity and AUC% of test compounds**

Compound	PRR_{50} (nM)			EC_{50} (nM)	AUC%		
	24 h	48 h	72 h		24 h	48 h	72 h
ACT-451840	2.77	2.72	4.07	1.95	89.2	95.6	90.6
Artemether	16.5	16.4	35.2	6.34	87.1	88.2	77.3
DHA	3.36	4.13	11.8	2.05	94.2	93.9	81.8
Cipargamin	1.61	1.17	1.15	1.29	88.6	98.2	100.1
DDD-107498	2.70	3.12	3.67	0.84	76.1	84.0	85.0
Chloroquine	16.9	11.3	10.4	4.85	78.6	86.6	89.1
Ganaplacide	117.5	30.0	15.9	7.05	55.1	71.9	80.0
Lumefantorine	24.7	15.3	15.0	7.28	67.9	67.4	66.7
Mefloquine	52.9	54.5	66.7	15.9	76.1	72.3	71.7
MMV048	276.9	209.6	23.5	23.9	62.6	72.1	78.3
Atovaquone	124.9	15.0	20.8	0.57	49.5	51.4	46.9
DSM265	1186	211.5	332.4	5.84	50.6	51.7	50.2
ELQ-300	9990	139.3	298.5	24.8	40.3	56.9	48.5
Pyrimethamine	9990	9990	9990	15.3	10.1	21.5	0.00
Cytochalasin D	9990	15.9	24.1	20.5	24.7	65.3	86.8

539 PRR_{50}: Concentration of the compounds required to reduce the PRR values to 50%; EC_{50}:

540 effective concentration to reduce the parasite growth to 50%; AUC: area under the curve; DHA:

541 dihydroartemisinin

542

543 **Figures**

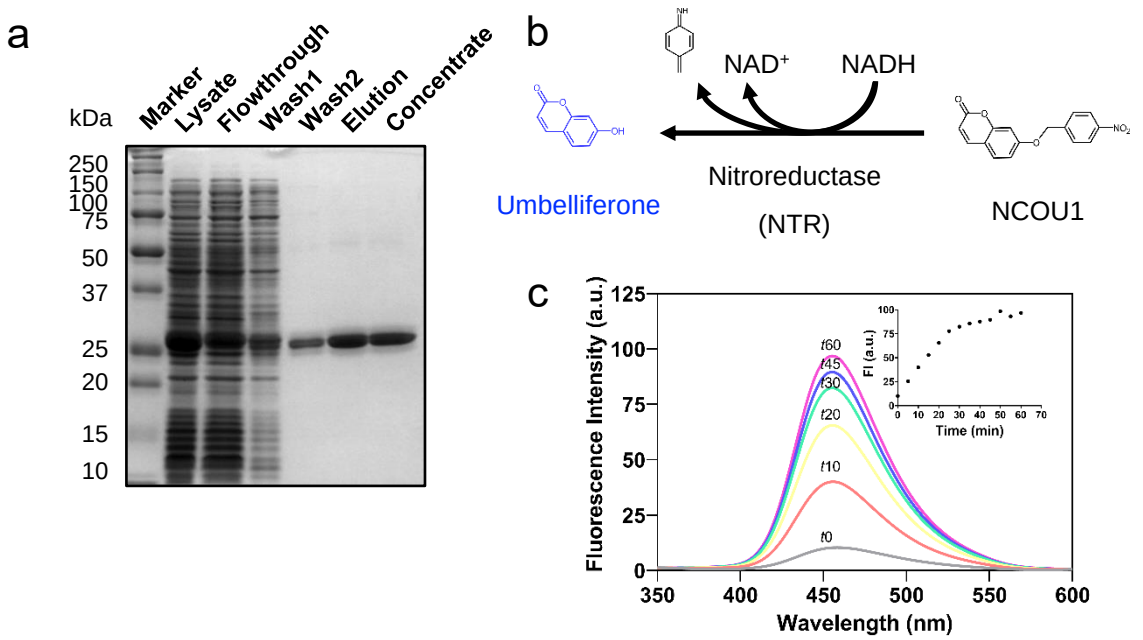

544 **Figure 1. Purification of recombinant nitroreductase (NTR) and quantification of**

545 **enzymatic activity. a** Recombinant C-terminally His_{10}-tagged NTR was expressed in *E. coli* BL21

546 Star (DE3) and purified using Ni-NTA agarose. In the lanes denoted as Marker, Lysate,

547 Flowthrough, Wash1 and Wash2, a total of 10 μg protein were loaded. For Elution and

548 Concentrated lanes, 2 μg were loaded. Estimated protein size is 26.7 kDa. **b** Scheme of the

549 enzymatic reaction catalyzed by NTR reducing NCOU1 to umbelliferone ($\lambda_{ex/em}$ = 315/455 nm).

550 **c** The fluorescent spectra of umbelliferone. Time-dependent increases in the fluorescence

551 spectra were recorded for 60 minutes at room temperature in NTR assay buffer (30 mM Tris-

552 HCl, pH 8.0, 0.25 % Triton X-100) containing 5 μg/mL NTR, 20 μM NCOU1, and 50 μM NADH

553 ($\lambda_{ex/em}$ = 315/350–600 nm over 0.5-nm intervals, recorded every 5 minutes). For better

554 visualization, only the spectra from time points at 0, 10, 20, 30, 45, and 60 minutes are shown

555 (grey: 0 min, orange: 10 min, yellow: 20 min, light blue: 30 min, blue: 45 min, purple: 60 min).

556 Fluorescence intensity (FI) over time ($\lambda_{ex/em}$ = 315/455 nm) is plotted in the inset. NCOU1:

557 nitrobenzyl-umbelliferone 1, NAD^+: oxidized nicotinamide adenine dinucleotide, NADH:

558 reduced nicotinamide adenine dinucleotide, a.u.: arbitrary unit.

559

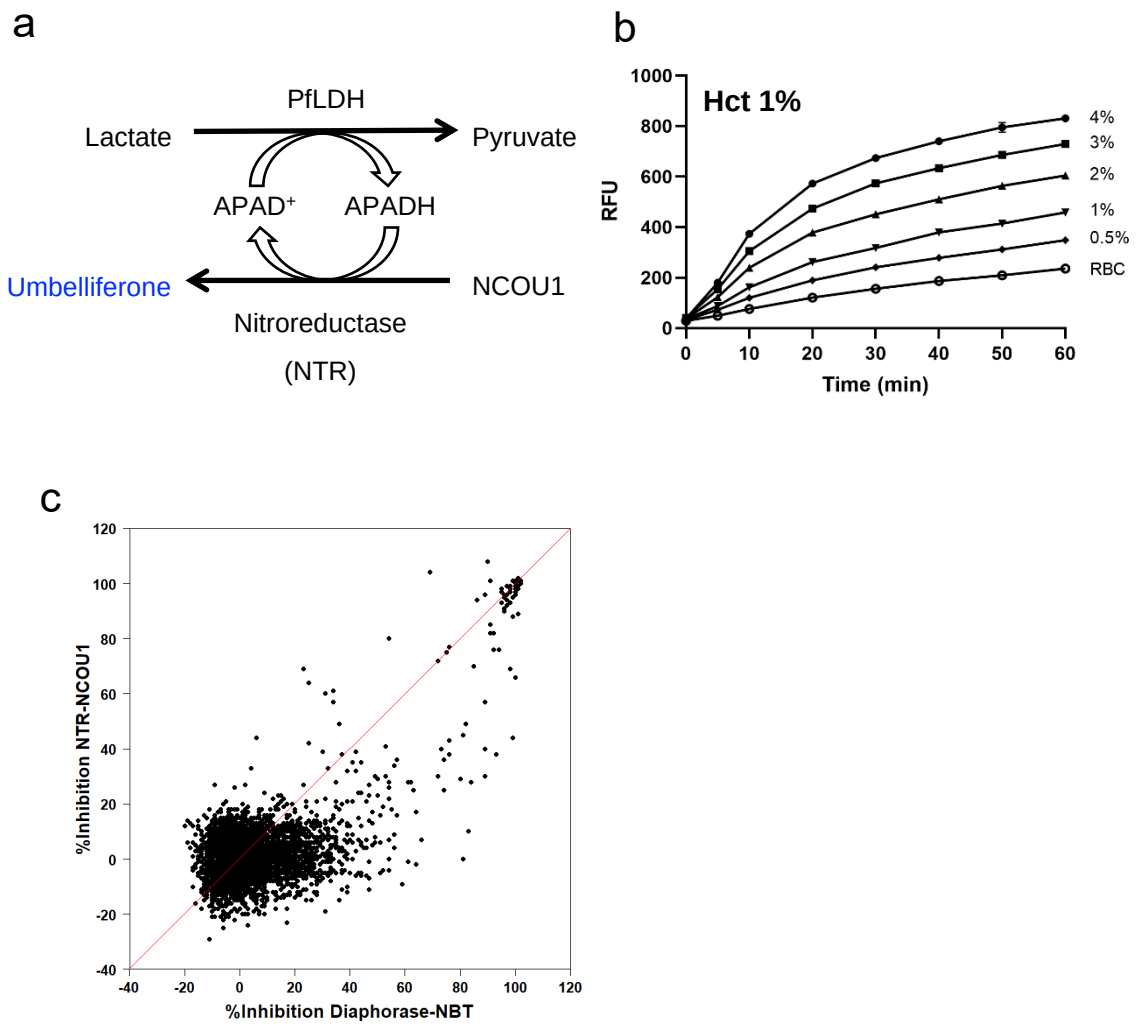

Figure 2. Novel assay using nitroreductase (NTR) coupled with *Plasmodium falciparum* lactate dehydrogenase (PfLDH).

a Scheme of the PfLDH-NTR coupled reaction used for quantification of parasite growth using NCOU1 as the NTR probe. **b** Parasitemia titration measured by the NTR-NCOU1 assay. The umbelliferone signal increased in a parasitemia-dependent manner. Each parasite culture (1% haematocrit (Hct)) was assayed with PfLDH buffer (100 mM Tris-HCl (pH 8.0), 150 mM lithium L-lactate, and 0.25 % Triton X-100) containing 100 μM $APAD^+$, 100 μM NCOU1, and 0.05–0.1

567 U/mL NTR at room temperature. **c** Correlation of %Inhibition between conventional

568 diaphorase-NBT and NTR-NCOU1 assays of PfLDH activity. The red line indicates unity (y = x).

569 NCOU1: nitrobenzyl-umbelliferone 1, $APAD^+$: oxidized 3-acetylpyridine adenine dinucleotide,

570 APADH: reduced 3-acetylpyridine adenine dinucleotide, RFU: relative fluorescence units. RBC:

571 red blood cell.

572

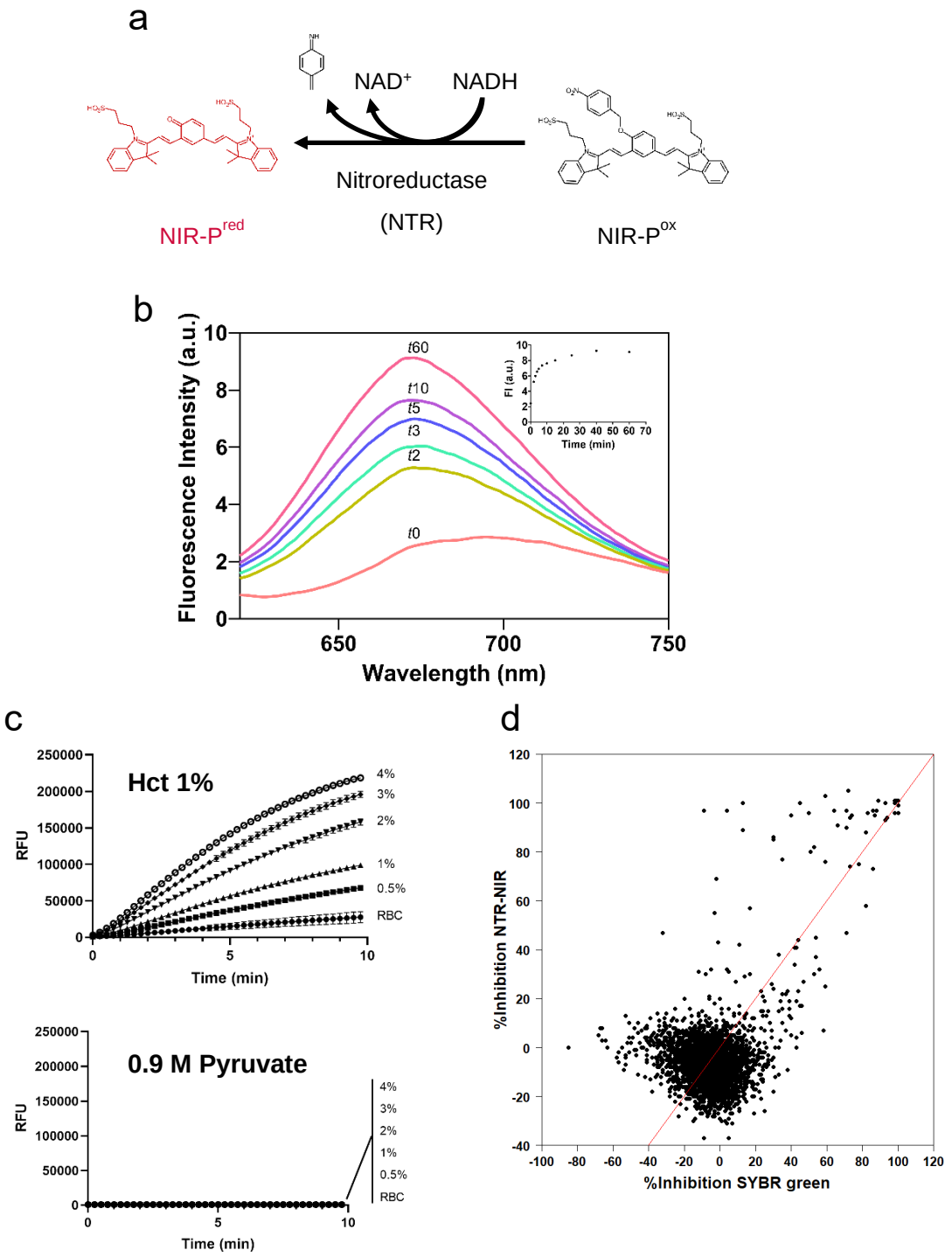

573 **Figure 3. Nitroreductase (NTR) assay using near-infrared probe (NIR-P). a** Scheme of

574 enzymatic reaction of NTR and NIR-P^{ox} producing the fluorescent NIR-P^{red} ($\lambda_{ex/em}$ = 615/670

575 nm**). b** Time-dependent fluorescent spectra of NIR-P^{red} produced by NTR. The enzymatic

576 reaction catalyzed by NTR was monitored using 50 μM NIR-P^{ox} and 50 μM NADH in 30 mM Tris-
577 HCl, pH 8.0, buffer containing 0.5 μg/mL NTR. Fluorescence signals ($\lambda_{ex/em}$ = 605/620–740 nm
578 over 1-nm intervals) were measured over a 60-minute period at room temperature (orange: 0
579 min, yellow: 2 min, light green: 3 min, blue: 5 min, purple: 10 min, red: 60 min). Fluorescence
580 intensity (FI) over time is plotted in the inset. Note that the reduction of NIR-P by NTR is much
581 faster than the reaction observed using the NCOU1 substrate (Fig. 1c). **c** Parasitemia titration
582 measured using the NTR-NIR assay. Each parasite culture (1% haematocrit (Hct)) was assayed
583 in PfLDH buffer (100 mM Tris-HCl, pH8.0, 300 mM lithium L-lactate, and 0.25% Triton X-100)
584 containing 500 μM $APAD^+$, 200 μM NIR probe, and 0.05 U/mL NTR at room temperature. The
585 quenching ("stop") solution consisted of 0.9 M pyruvate. Data are presented as the mean ±
586 standard deviation (SD) (n=4). **d** Correlation of %Inhibition between conventional SYBR green
587 and NTR-NIR assays of PfLDH activity. The red line in the graph represents the line of equality
588 (y = x). a.u.: arbitrary unit, NAD^+: oxidized nicotinamide adenine dinucleotide, NADH: reduced
589 nicotinamide adenine dinucleotide, RFU: relative fluorescence units.
590

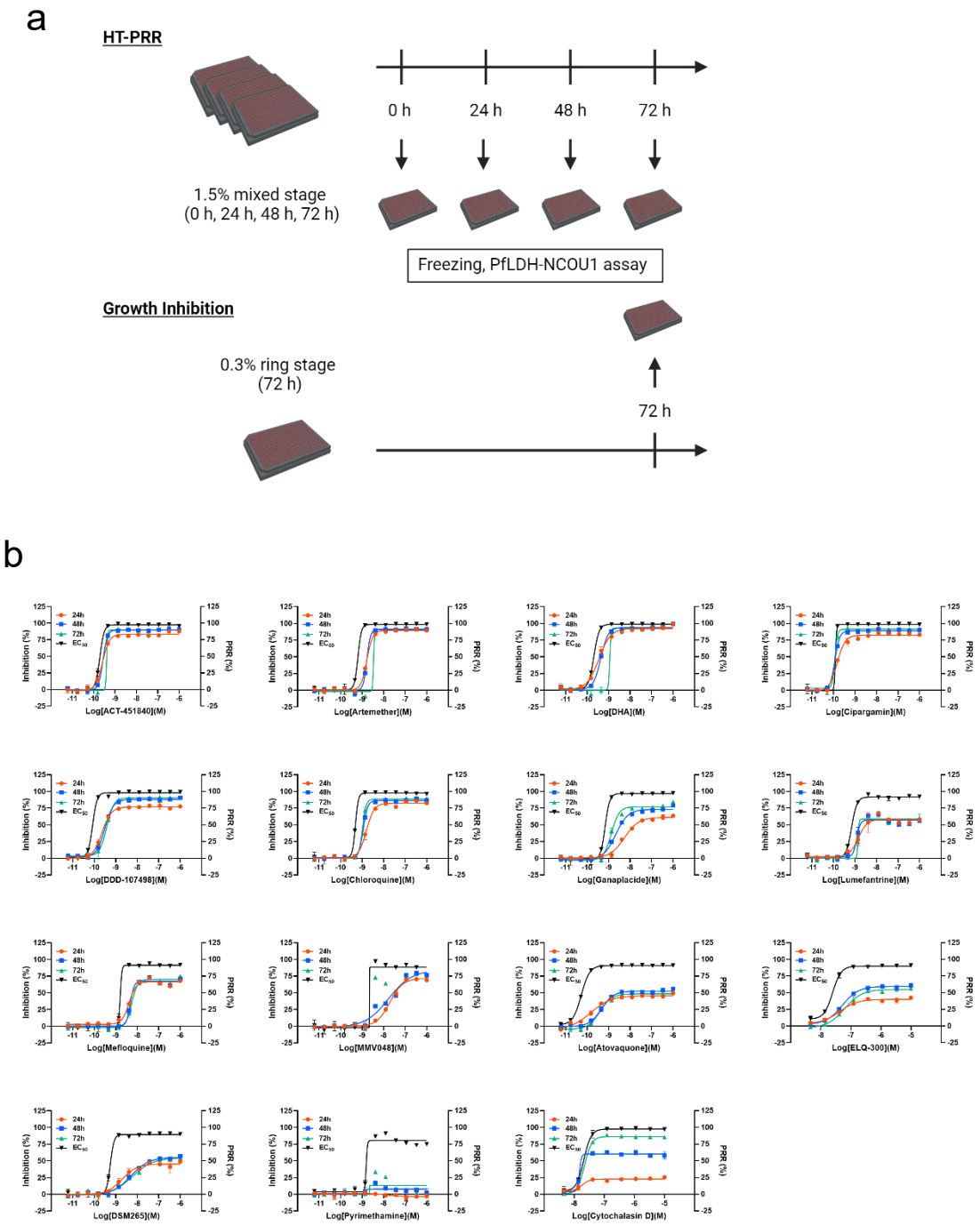

591 **Figure 4. Schematic representation of high-throughput parasite reduction ratio (HT-PRR)**

592 **and assessment of well-characterized antimalarial agents. a** To evaluate the parasite

593 reduction ratio (PRR) by established HT-PRR methods, non-synchronized 3D7 parasites

594 (haematocrit (Hct) 1%, parasitemia 1.5%) were plate-cultured for 0, 24, 48, and 72 hours in the
595 presence of compound. For the growth inhibition assay, 3D7 parasites were synchronized by
596 exposure to 5% sorbitol; ring stage parasites then were plate-cultured for 72 hours in the
597 presence of compound. Growth was terminated at the indicated time point by freezing (at -30 °
598 C) the respective assay plates; the number of live parasites then was quantified via an LDH assay
599 using retororeductase (NTR) and nitrobenzyl-umbelliferone 1 (NCOU1). For the growth
600 inhibition assay, the positive control consisted of a mixture of 1 μM atovaquone and artemisinin;
601 the negative control consisted of 0.4% dimethylsulfoxide (DMSO). For the HT-PRR assay, the
602 positive and negative controls consisted of 1 μM dihydroartemisinin (DHA) and 0.4% DMSO,
603 respectively. **b** Dose-response curves of Inhibition (%) and PRR (%) by test compounds were
604 generated for each assay condition (n =2).